Pozzolanic Performance of Ceramic Sludge Ash (CSA) Modified-Cement Pastes

HHM Darweesh*

Department of Refractories, Ceramics and Building Materials, National Research Centre, Egypt
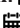
Abstract

Ceramic Sintered Sludge Ash (CSSA) has garnered a great attention for its potential to mitigate CO_2 emissions by its replacing into cement. This study investigates the consequential changes in the properties of cement paste blended with CSSA. Laboratory tests indicated that the high specific surface area of CSSA was the essential factor contributing the increase of water of consistency and the delaying of setting time. In terms of strength, the CSSA affected the cement paste to a greater extent after 3 days of hydration than at 28 days. The inert hydration components as quartz and feldspar in CSSA may be responsible for the observed early hydration retardation. During 28 days of hydration, physical and mechanical properties were employed to quantify $Ca(OH)_2$ content and the degree of cement hydration. The participation of CSSA in the pozzolanic reaction could additionally produce calcite, which promoted hydration and improved the strength of cement paste up to 90 days. Scanning electron microscopy (SEM) revealed that amorphous hydration products, CSHs and $Ca(OH)_2$ covering the CSSA surface, were observed forming a robust structure due to normal hydration and pozzolanic activity of CSSA.

Keywords: Ceramic sintered sludge ash; Cement paste; Consistency; Setting; Water absorption; Density; Porosity; Strength; Free lime; Heat of hydration; SEM

Introduction

Carbon dioxide emission (CO_2) during the manufacture of cement is the main anthropogenic contributor to global warming [1-3]. Global warming may lead to human casualties and substantial economic losses [3,4]. Against the backdrop of global efforts to reduce CO_2 emissions from cement, Dredged Sludge (DS) has emerged as a widely studied supplementary cementitious material (SCM), aiming to partially replace cement in the formulation of cement paste [5-8]. This is particularly relevant as clinker, a pivotal cement component, shares similar compositions with Sintered Sludge Ash (SSA) [9-12]. At present, some scholars have studied the working performance of SSA. The rough surface and porous structure of SSA particles demonstrated its reduced fluidity in cementitious mortar [13-15]. The study identified an average 6% reduction in the fluidity of cement pastes for every 10% increase in SSA substitution rate. Another research studies indicated that SSA delayed the setting of cement pastes [16-20]. Notably, the cement dilution effect predominantly impacts the early strength of cementitious mortar but has a minimal influence on the long-term strength [21-23]. As the hydration process advances, the pozzolanic reaction of SSA with $Ca(OH)_2$, is generating additional hydration products that compensate for the initial strength loss [24,25]. The early strength reduction is mainly attributed to the inhibition of the early hydration reaction by orthophosphate from SSA in the pore solution [26]. The presence of other hydration inert substances in SSA involving mineral composition characterization and analysis might be effective. This is the main cause that influencing the early hydration, The pozzolanic reactions during the later ages of hydration showed that SiO_2-rich SCM affected the amount and type of the formed hydration products. This subsequently influenced the properties of cements such as fluidity, porosity and strength. This is essentially attributed to

that SiO_2 in alkaline environments easily react with $Ca(OH)_2$. Thus, SSA is precisely rich in SiO_2, Al_2O_3 and CaO [27-30]. Therefore, it appears both effective and necessary to investigate the impact of SSA on the long-term strength of cement paste by examining the reactants and products of the pozzolanic reaction [31-35]. Currently, common indexes for evaluating the pozzolanic reaction include heat release, bound water, and/or $Ca(OH)_2$ consumption serves as a reliable indicator [28-32]. They showed that the relationship between heat release and $Ca(OH)_2$ consumption depended on the chemical composition of the pozzolan itself. The objective of the current study is to evaluate the effect of the CSSA waste material on the various properties of the OPC pastes. The results are confirmed by measuring the free lime content, heat of hydration and Scanning Electron Microscopy (SEM).

Experimental

Raw materials

The main raw materials used in the present study are Portland cement (OPC) which was delivered from Sakkara cement factory, Giza, Egypt. The elementary phases of the OPC are tabulated in Table 1, while the oxide ratios of the OPC and Ceramic Sludge Ash (CSA), as measured by an X-ray Fluorescence Spectrometer (XRF) are summarized in Table 2. The basically physical properties of the used OPC cement and CSA are shown in Table 3. The CSA was first dried in a drying oven and kept at 100 °C for 48 hours. The CSA was calcined in a furnace up to 800 °C for 2 hours. Then, it was put into a ball mill for 2 min to obtain CSA [23-25]. The particle size distributions of the OPC and SSA are shown in Figure 1, where the CSA is the higher fineness, whereas the OPC is the lower. Table 4 shows the constitutions of the various cement mixtures. The CSA was substituted for cement to prepare cement mixtures.

Table 1: Mineralogical composition of OPC sample, wt. %.

Phase Material	C_3S	β-C_2S	C_3A	C_4AF
OPC	46.81	28.43	5.90	12.56

Table 2: Chemical composition of materials (%).

Oxides Materials	SiO_2	Al_2O_3	Fe_2O_3	CaO	MgO	Na_2O	K_2O	SO_3	LOI	Total
OPC	20.58	5.03	3.38	63.32	2.01	1.23	0.68	2.06	1.76	
CSA	56.12	17.26	7.88	9.22	3.29	.0.96	2.98	1.60	1.65	

Table 3: Physical properties of the raw materials, wt. %.

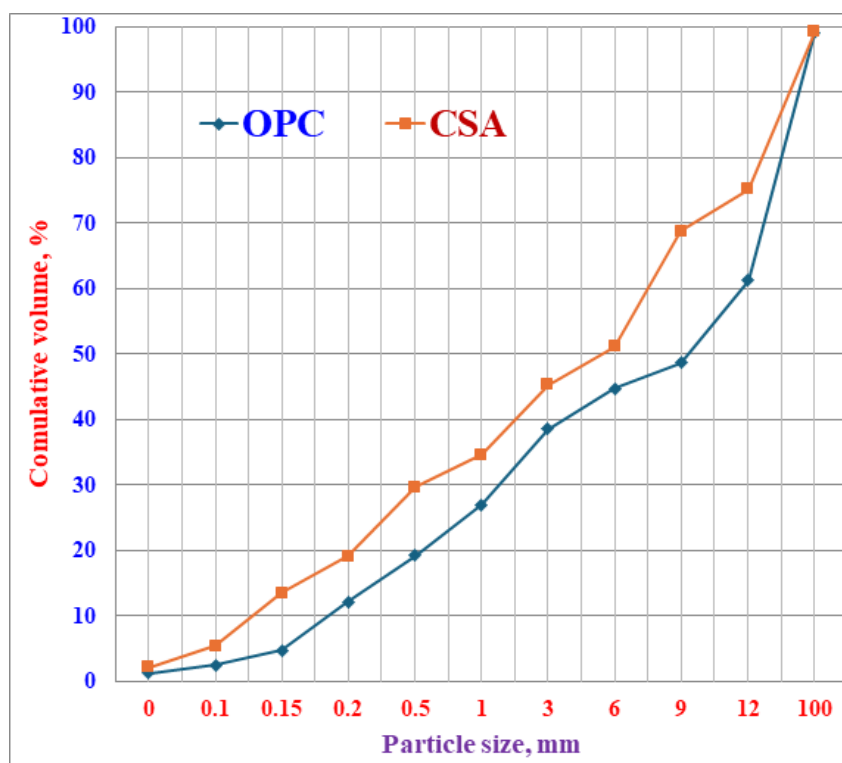| Properties Materials	Specific gravity	Density, g/cm³	Blaine surface area, cm²/g
OPC	3.15	3.12	3564
CSSA	2.66	2.87	5683

Figure 1: Particle size distribution of raw OPC and CSA.

Table 4: Composition of cement mixtures, wt. %.

Mixtures Materials	S0	S1	S2	S3	S4	S5	S6	S7
OPC	100	95	90	85	80	75	70	65
CSSA	0	5	10	15	20	25	30	35

Preparation and methods

During the preparation of cement mixtures, different dosages of CSA (0, 5, 10, 15, 20, 25, 30 and 35 wt. %) were added to the OPC. These OPC/CSC mixtures were categorized into nine groups as S0, S1, S2, S3, S4, S5, S6 and S7, respectively. The blending process of the various cement blends was done in a porcelain ball mill containing 2-4 balls for two hours to assure the complete homogeneity of all cement blends. Firstly, the water of consistency (w/c- ratio) and setting time are measured using Vicat apparatus [36-38]. The cement pastes were then cast using the predetermined water of consistency, i.e. during mixing, the right w/c-ratio was poured into the cement portion inside the mixer and then run the mixer for about 5 minutes at an average speed of 10rpm in order to have a perfect homogenous mixture, moulded into one inch cubic stainless steel molds of dimensions $2.5 \times 2.5 \times 2.5cm^3$ using about 500g cement mix, vibrated manually for three minutes and then on a mechanical vibrator for another three minutes [31]. The surface of the molds was smoothed using a suitable spatula. Thereafter, the molds were kept in a humidity chamber for 24 hours under 95 ± 2RH and room temperature of 20 ± 2 °C for curing until the corresponding days, demolded in the next day and soon immersed in water till the time of testing at 1, 3, 7, 28 and 90 days. Water absorption, bulk density and apparent porosity [39,40] of the hardened cement pastes could be calculated from the following relations:

$$WA, \% = (W1-W2) / (W3) X 100 \quad (1)$$

$$BD, g/cm^3 = (W1) / (W1-W2) \quad (2)$$

$$\varepsilon = (0.99 \times We \times BD) / (1+Wt) \quad (3)$$

Where, W1, W2, W3, ε, We and 0.99 are the saturated, suspended, dry weights, total porosity, free or evaporable water content and specific volume of free water, respectively.

Flexural strength (FS) was calculated [41,42], whereas the samples were marked at three points adjusting to place them on the correct point of contact (Figure 2). Then, the FS was obtained from the following equation: -

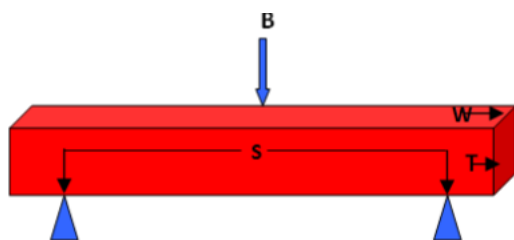$$FS = 3 (PL) / 2 (b) (d) / 10.2 (MPa) \quad (4)$$

Figure 2: Schematic diagram of bending strength, B: Beam or loading of rupture, S: Span, W: Width and T: Thickness.

Where, L: load taken, P: bean or loading of rupture, b: width, d: thickness.

The compressive strength [43,44] from the following relation:

$$Cs = L (KN) / Sa (cm^2) KN/m^2 x 102 (Kg/ cm^2)/10.2 (MPa) \quad (5)$$

Where, Cs: Compressive strength (MPa), L: load (KN), Sa: surface area (cm^2).

The chemically-combined water content at each hydration age was also determined on the basis of ignition loss [31,32,45,46] as follows:

$$Wn, \% = W1-W2 / W2 x100 \quad (6)$$

Where, Wn, W1 and W2 are combined water content, weight of sample before and after ignition, respectively. The free lime contents (FLn) of the hydrated samples pre-dried at 105 °C for 24h were also measured [31,44,45,47,48]. The X-ray Fluorescence (XRF) was used to analyze the chemical and mineralogical composition of OPC and CSSA raw materials, identifying crystalline phases of OPC cement. Subsequently, based on the quantitative analysis of Ca $(OH)_2$ consumption and the degree of cement hydration was conducted to explore the effect of CSSA on the long-term strength of cement pastes. Meanwhile, scanning electron microscopy (SEM) was conducted to explore the microscopic morphology and pore size distribution of CSSA to provide a basis of promoting its application. The phase compositions of some selected samples were investigated using Infrared Spectroscopy (IR) and Scanning Electron Microscopy (SEM). The IR spectra were performed by Pye-Unicum SP-1100 in the range of 4000-400cm^{-1}. The SEM images of the fractured surfaces, coated with a thin layer of gold, were obtained by JEOL-JXA-840 electron analyzer at accelerating voltage of 30KV. Each group comprised three specimens where the arithmetic mean was considered for each group to determine the corresponding strength values, noting that any abnormal data must be excluded.

Results and Discussion

Water of consistency and setting time

The Water of Consistency (WC) and Setting Times (ST) of the OPC cement pastes (S0) blended with various ratios of CSA (S1-S7) are shown in Figure 3. It is clear that the WC of the control (S0) was 28.83 %. This value was increased as the content of CSSA increased. On the other side, the ST (Initial and final) of the blank (S0) were 132 and 157min. respectively. These values were enhanced as the CSSA content increased. This is mainly contributed to the higher surface area or fineness of CSA material [49-52]. Moreover, the pozzolanic reactions of the CSA with the produced Ca $(OH)_2$ from the normal hydration process which in need of more water to occur [45,51-55].

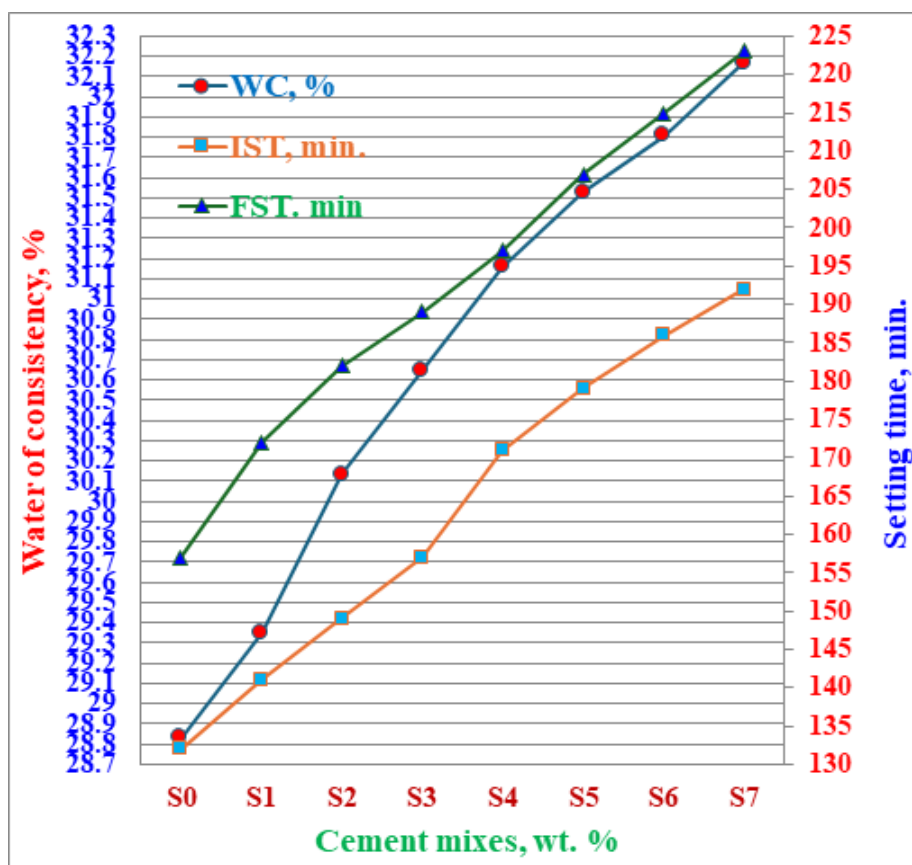**Figure 3:** Water of consistency and setting time of Portland cement pastes blended with CSA.
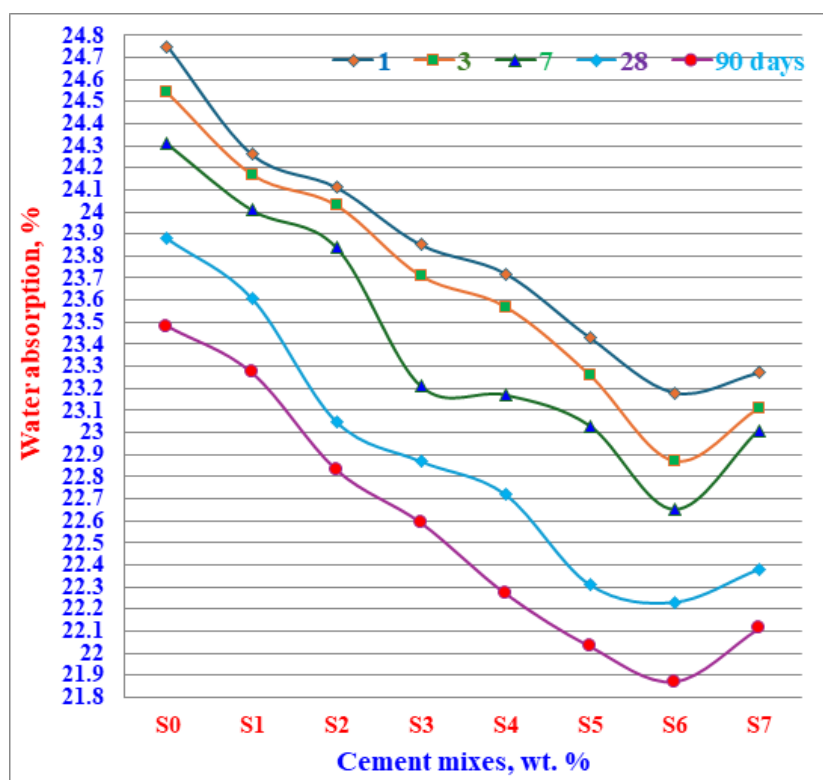
Physical properties

Figure 4: Water absorption of Portland cement pastes blended with CSA hydrated up to 90 days.

Water absorption: The results of Water Absorption (WA) of the OPC cement pastes blended with various ratios of CSA hydrated up to 90 days are represented in Figure 4. Results illustrated that the WA of the control (S0) gradually decreased all over the hydration times. This is mainly due to the normal hydration process of the cement phases [36,52,56]. As the CSA content increased, the WA decreased. This firstly may be attributed to the increased compaction of the hardened cement pastes as a result of the decreased pore structure, and moreover the pozzolanic property of the CSA with the resulting free lime, $Ca(OH)_2$ that is coming from the hydration of di- and tricalcium silicates phases of the cement [44,45,57]. This continued only up to 30 wt. % CSA (S6). But, with any further CSA addition, the water absorption tended to increase (S7). This is essentially contributed to that the higher content of

CSA at the expense of the main binding material (OPC) negatively reflected on the WA results [31,45,51-53,58-60]. Accordingly, the higher content of the additive material must be refused.

Bulk density: Figure 5 shows the bulk density (BD) of the cement mixtures with the CSA (1-8) compared to that of the control mixture (A0) hydrated up to 1, 14, 28 and 90 days. Results showed that the BD gradually increased as the content of CPSA increased [31,36,38,61]. This continued till the mix containing 30 wt. % (A6). With any increased addition of CSA › 30 wt. %, the BD tended to decrease. The increase of BD is due to the increased compaction by CSA which precipitated inside the pore volume of the samples. This resulted to decrease the total porosity [44,45,51,62]. So, the higher amounts of CSA must be avoided.
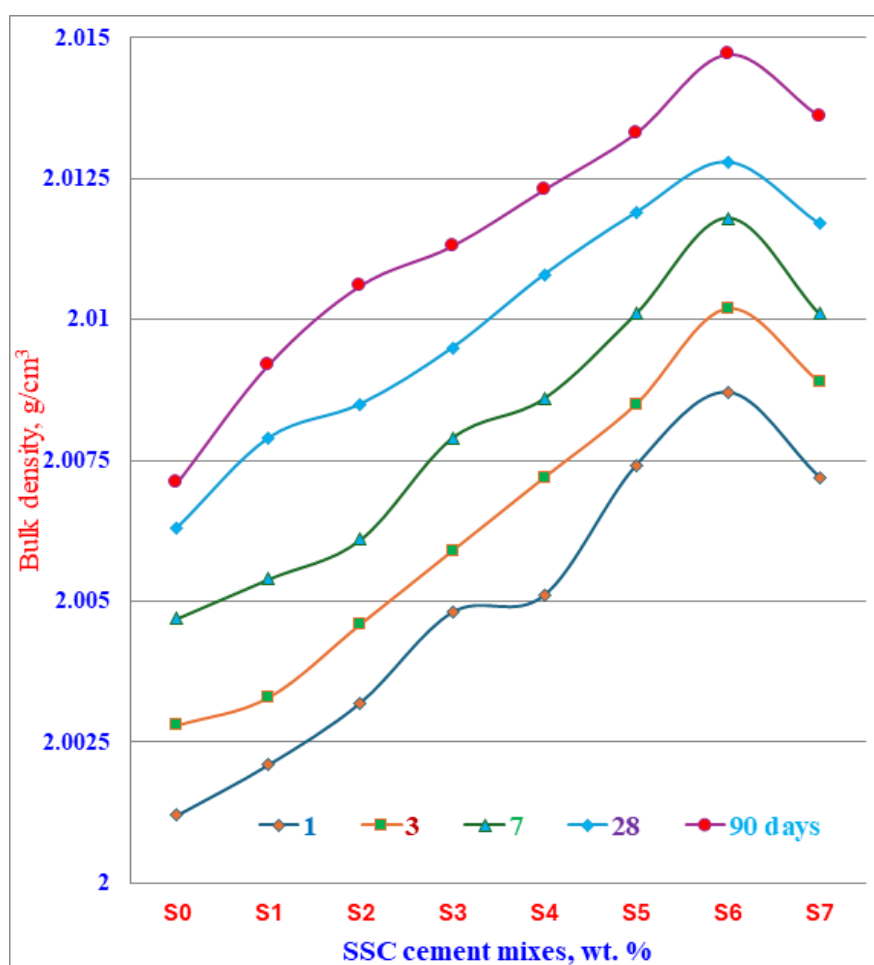

Figure 5: Bulk density of Portland cement pastes blended with CSA hydrated up to 90 days.

Total porosity: The results of total porosity (TP) of the OPC cement pastes (S0) blended with various proportions of CSA (S1-S7) hydrated up to 90 days are illustrated in Figure 6. As clearly shown by the figure, the TP decreased as hydration proceeded up to 90 days. Moreover, it decreased as the CSA content increased, but this continued only up to 30 wt. % (S6) and then increased with any further increase of CSA addition. The decrease in TP is essentially attributed to the pozzolanic properties of CSA with the evolved

$Ca(OH)_2$ from the hydration of C_3S during the early ages and C_2S during the later ages of hydration [21,36,46]. But the increased value of TP is mainly attributed to the delaying of hydration process due to the incorporation of larger amounts of CSA which in turn decreased not only the normal hydration process, but also the pozzolanic activity of CSA [63-65]. So, the higher amounts of CSA must be refused due to its adverse effect. The results of TP are agreed with those of WA to a large extent.
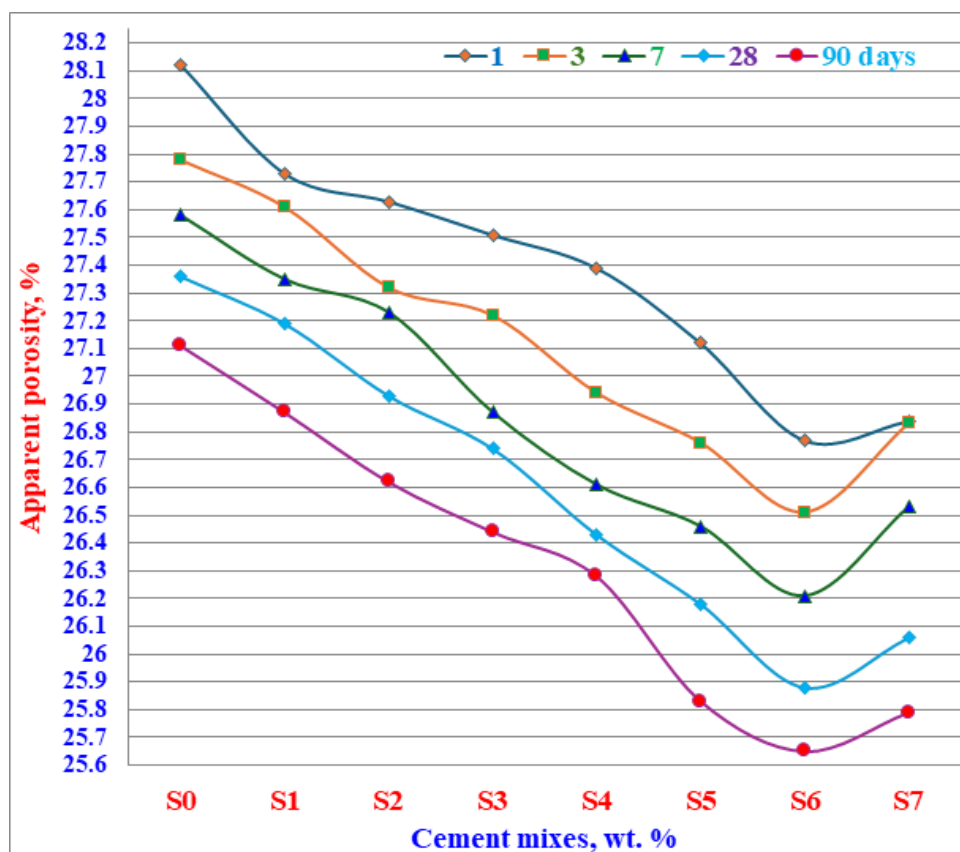
Figure 6: Total porosity of Portland cement pastes blended with CSA hydrated up to 90 days.

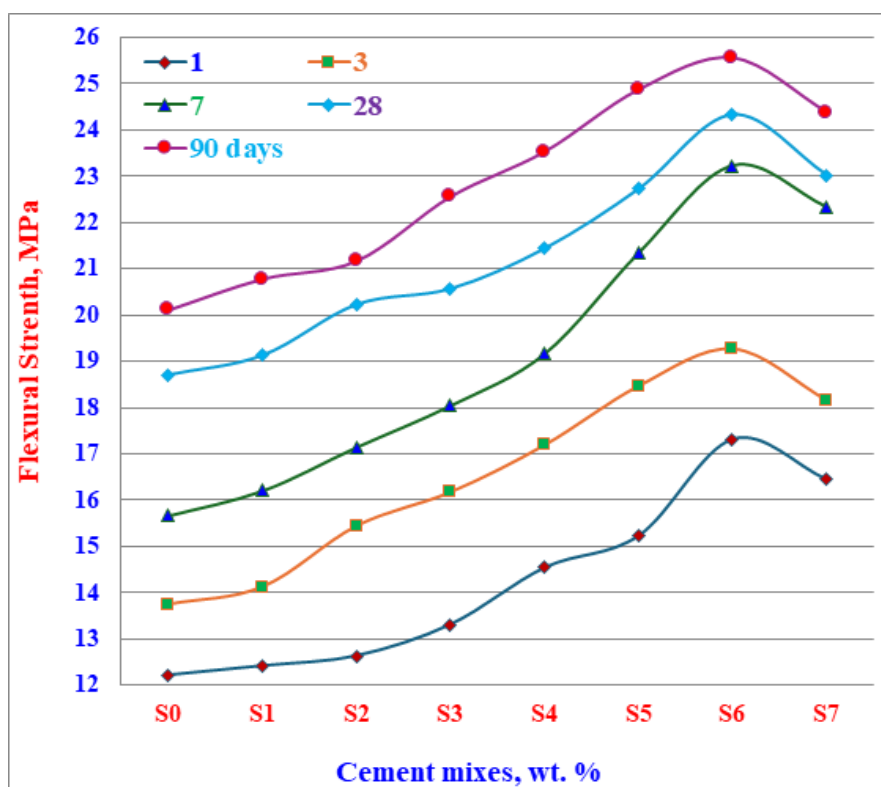**Mechanical properties**

Figure 7: Flexural strength of Portland cement pastes blended with CSA hydrated up to 90 days.

Flexural strength: The results of flexural strength (FS) of the OPC cement pastes (S0) blended with different ratios of CSA (S1-S7) hydrated up to 90 days are demonstrated in Figure 7. As shown from the figure, the FS increased as the hydration time increased up to 90 days. This is mainly contributed to the newly formed hydration products due to the normal hydration process, which in turn improved the FS of the hardened cement pastes [36,64]. The FS also improved and enhanced with the addition of CSA only up to 30 wt. % (S6), and then adversely affected by any further addition of CSA (S7). The increased FS results with CSA addition are often due to the pozzolanic reactivity of CSA with the released $Ca(OH)_2$ from the hydration process of di- and tricalcium silicates (C_3S and β-C_2S) of the cement. Moreover, the unreacted CSA acted as filler that closed the pore system of samples, i.e. the total porosity decreased [52,65,66]. The adverse results with the higher addition of CSA (S7) are mainly attributed to the higher amounts of additive material hindered the hydration of cement phases and helped to open the pore structure to a large extent [44-46]. Therefore, the higher amounts of CSA must be removed.

Compressive strength: The Compressive Strength (CS) of the hardened OPC cement pastes (S0) blended with different ratios of CSA (S1-S7) hydrated up 90 days are represented in Figure 8. The CS of all cement pastes increased as the hydration time proceeded up to 90 days. This is essentially attributed to the newly resulting hydration products or CSH which are deposited in the pore system, i.e. this decreased the total porosity and increased the bulk density. So, this reflected positively on the CS of the hardened cement pastes [36,44,62], and also the crystal growth of the formed CSH gradually improved and enhanced. The improvements of CS often enhanced with the addition of CSA, but only up to 30wt. % (S6), and then adversely affected with any further increase of CSA (S7). The improved CS results with CSA addition are often due to the pozzolanic reactions of CSA with the resulting $Ca(OH)_2$ that is coming from the normal hydration process of di- and tricalcium silicates (C_2S and C_3S) of the cement, Furthermore, the CSA improved the compaction of the constituents together, i.e. the pore structure was partially or completely closed, i.e. the unreacted CSA particles were acted as filler that closed the pore system of samples [50,65,66]. The adverse results with the higher content of CSA (S7) were mainly attributed to the higher amounts of the additive material hindered and largely stopped the hydration of cement phases and helped to open more-pore structure to a large extent [31,44-46]. Therefore, the higher contents of CSA must be illuminated.
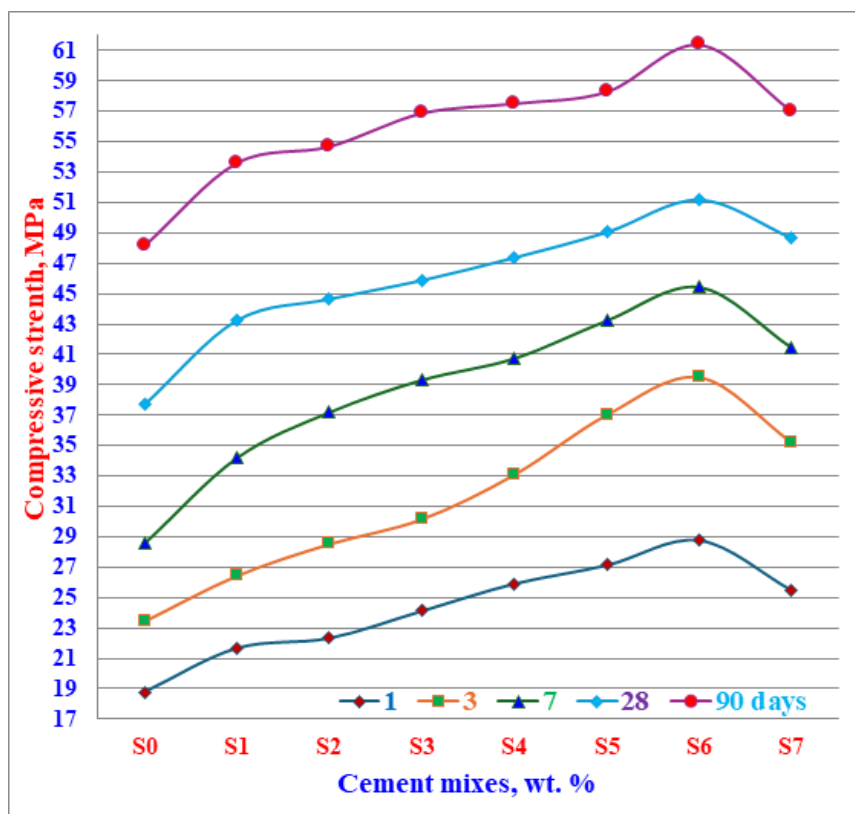

Figure 8: Compressive strength of Portland cement pastes blended with CSA hydrated up to 90 days.

Free lime content

The free lime contents (FLn) of the OPC cement (S0) blended with various ratios of CSA (S1-S8) hydrated up to 90 days are shown in Figure 9. The FLn of the control (S0) was gradually increased as the hydration time progressed up to 90 days. This is mainly attributed to the normal hydration process of the main silicate phases of the cement [36,53,67-69] as follows: -

$$3\ C_3S + 6\ H_2O \rightarrow C_3S_2H_3 + 3\ Ca\ (OH)_2\ (8)$$

$$2\ \beta\text{-}C_2S + 4\ H_2O \rightarrow C_3S_2H_3 + Ca(OH)_2\ (9)$$
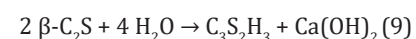
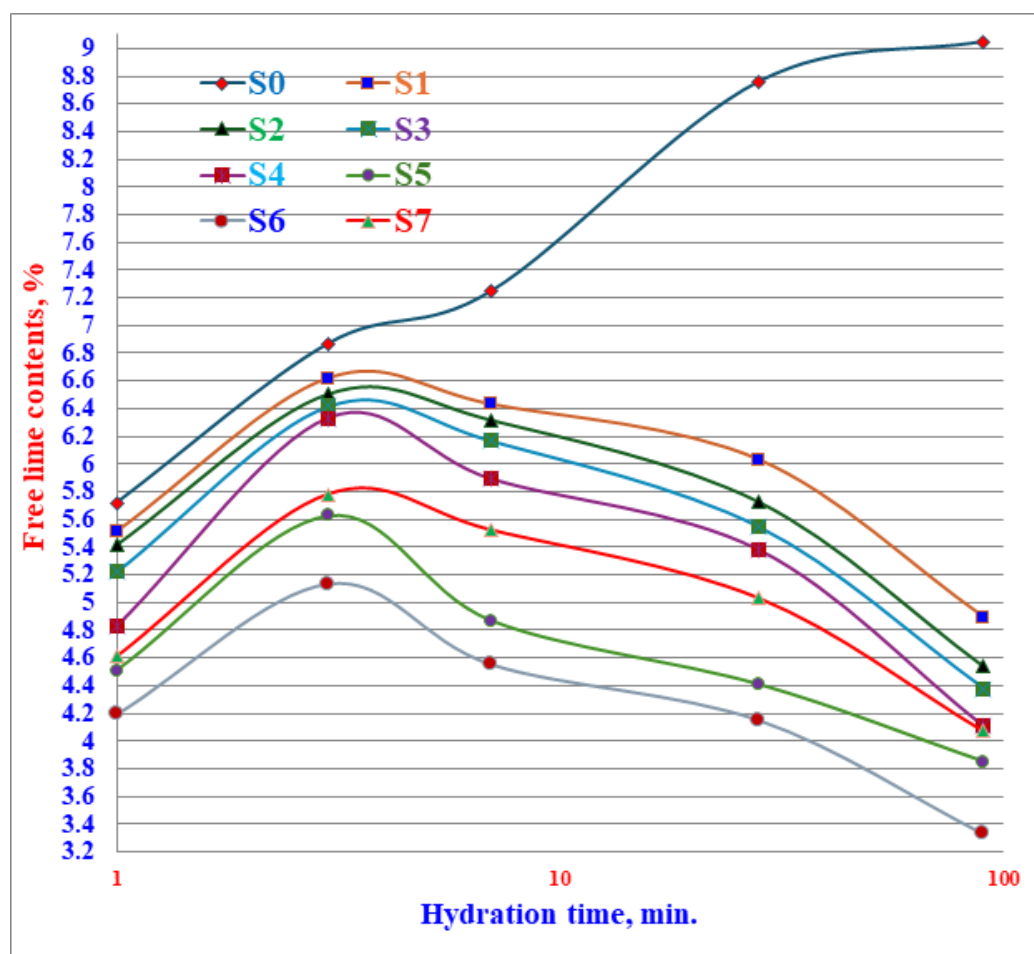**Figure 9:** Free lime contents of Portland cement pastes blended with CSA hydrated up to 90 days.

On the other side, the FLn of the other blended cements incorporated different ratios of CSA increased up to 7 days of hydration but then started to decrease down to 90 days. This is essentially due to the pozzolanic phenomenon that could be taken place between the resulting free line and CSA particles [59-61,68]. The consumption of FLn by its reaction with the constituents of CSA had led to the formation of additional CSH phases which precipitated into the pore structure of the hardened cement pastes. This in turn supported and improved the physical, chemical and mechanical properties. This was contributed to the improvements of the densification parameters and the microstructure due to the reduction of voids, porosity, and water permeability [31,44,45,67]. The FLn of cement pastes incorporated CSA › 30wt. % (S7) continued to decrease due to the high content of CSA at the expense of the OPC hindered its hydration, i.e. the hydration process was completely ceased.

Heat of hydration

Figure 10 shows the heat of hydration (HH) of the OPC cement pastes (S0) blended with different ratios of CSA (S1-S7) hydrated up to 90 days. As soon as the various cement powders become in contact with water, the heat of hydration starts to generate at once. The heat of hydration of all cement pastes was generally increased with the hydration time up to 28 days, but so slightly at later stages that it seemed to be constant. The same trend was displayed by all cement pastes incorporated different ratios of CSA [70-73]. This is essentially attributed to the increase of hydration level of cement phases that was coming from the pozzolanic reactions of CSA. This was accompanied by a gradual generation of heat [74-76]. Moreover, the rate of the generated HH was sharply enhanced at early ages from 3 up to 7 days. This is due to the activation effect on the hydration reaction mechanism of C_3S by the very fine CSA particles. At later ages (28-90 days), the rate of hydration reaction as well as the evolved HH increased so slightly that it seemed to be unchanged or stable. This may be due to the non-activation effect of C_3S and the slight activation action mechanism of β-C_2S at later ages. Also, the HH slightly enhanced as the CSA content increased, but only up to 30wt. % (S6). The increased values of HH are mainly due to two hydration mechanisms. The first is the normal hydration of the cement, while the second is the pozzolanic reactions of CSA with the resulting $Ca(OH)_2$ from the first process [70,71,74,75]. The HH was then unchanged with any further increase of CSA addition (S7). This is essentially contributed to the dilution effect of the CSA on the cementitious compounds and the high silica content of CSA. So, the high CSA content must be avoided due to its adverse action [72-76].
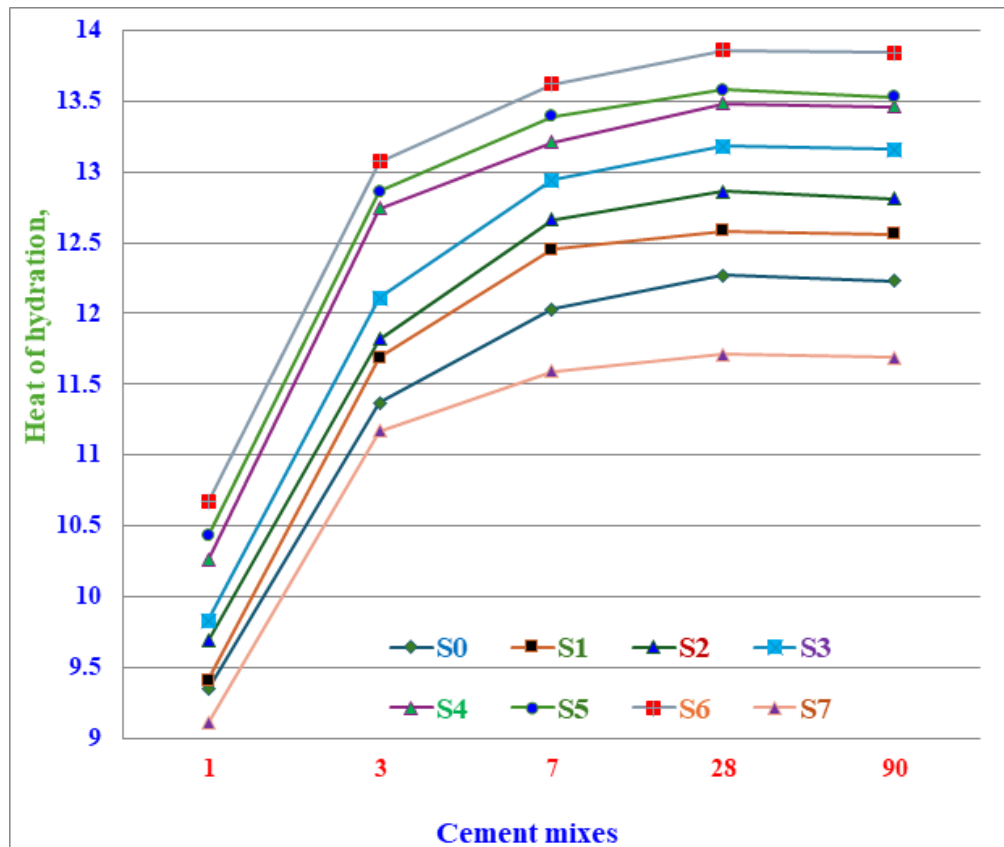
Figure 10: Heat of hydration of Portland cement pastes blended with CSA hydrated up to 90 days.

SEM spectra

The Scanning Electron Microscopy (SEM) of the OPC pastes blended with different ratios of CSA (A, B, C and D) or S0, S3, S6 and S7) hydrated up to 90 days is demonstrated in Figure 11. In image A of the blank (S0), ettringite phase was clearly shown as needle-like crystals and pits of free lime covered the surfaces of CSSA particles that had resulted from the normal hydration process. Also, crystals of CSH were formed. In image B (S3), the crystals of CSH and piles of free $Ca(OH)_2$ were increased, but the ettringite phase was clearly decreased. In image C (S6), it was full of CSH and no pits of free lime, while the ettringite phase was completely disappeared. In image D (S7), there are some internal cracks were noted and the reappearance of a very small amount of free lime which negatively reflected on the physical and mechanical properties. Moreover, the porosity was gradually decreased till S6 with the lowest degree of porosity. So, the cement batch (S6) could be considered the optimum one with well-developed crystal growth.
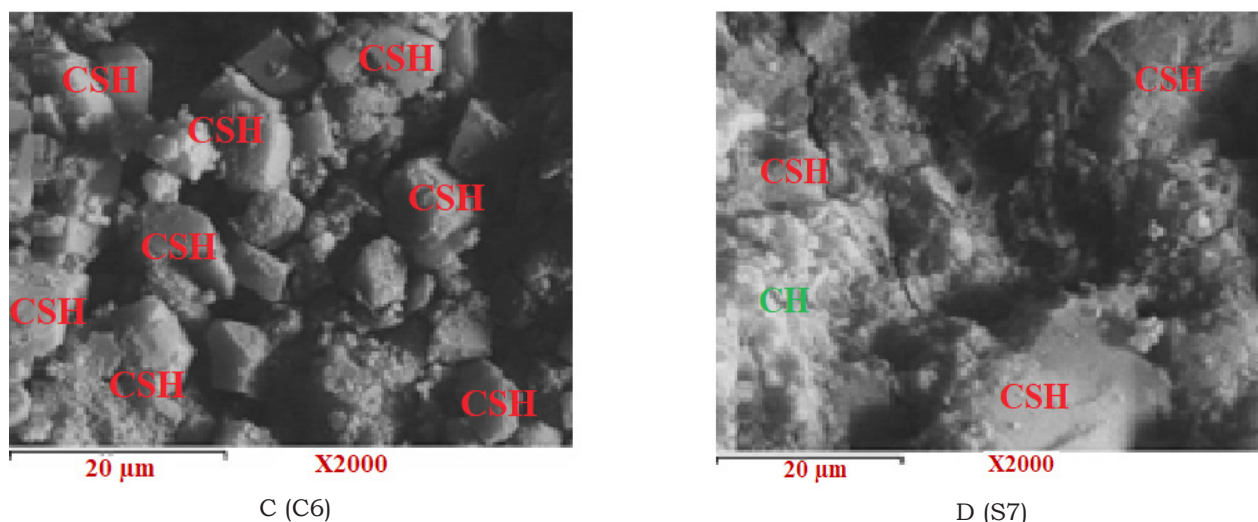

A (S0)

B (S3)

C (C6)

D (S7)
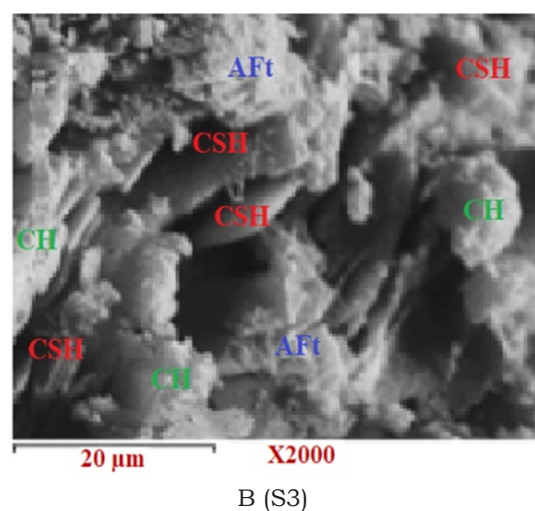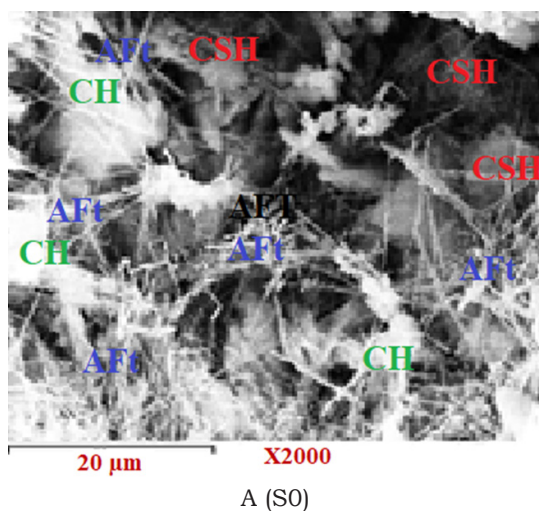
Figure 11:

Conclusion

The pozzolanic performance and characteristics of CSA were assessed. The CSA needs more water to produce good cement pastes, i.e. the w/c- ratio continuously increased causes. Also, it causes gradual retardation in both initial and final setting times, i.e. as the CSA content increased, the retardation time increased too. The CH content in the cement paste with 0% CSA on 90 days was approximately 9.05%, but this result significantly decreased with increasing of both curing time and CSA content. So, CSA is a pozzolanic material. As it is clear, the added CSA › 30wt% (S7), the CH content starts to increase due to the stopping of pozzolanic effect of the added material. The physical properties of cement pastes containing CSA material were improved and enhanced with curing time and CSA content, but only up to 30wt%. The flexural and compressive strengths of the blended cement increased as CSA content increased up to 30wt%. Any further increase of CSA content › 30 wt. %, the physical and mechanical properties would be diminished. So, the optimal CSA content that can be added to cement without adversely affecting its properties is 30wt%. SEM spectra revealed a higher quantity of CSHs in the CSA paste, resulting in a denser and more compact microstructure. The incorporation of large CSA content reduced the heat of hydration and prolonged the time required to reach the silicate and aluminate reaction. This was leading to delay hydration, which in turn resulted in extended setting times and reduced early and late strength development. The CSA powder contains SiO_2 and Al_2O_3 › 90% of its total mass, and therefore it has a natural of pozzolanic materials. Blending CSA with OPC could enhance the pozzolanic performance forming additional CSH-gel because it improves the densification parameters of the OPC pastes, i.e. it reduced the voids, porosity, and water permeability.

References

1. Geng Y, Wang Z, Shen L, Zhao J (2019) Calculating of CO_2 emission factors for Chinese cement production based on inorganic carbon and organic carbon. Journal of Cleaner Production 217: 503-509.

2. Wang L, Chen L, Provis JL, Tsang DCW, Poon CS (2020) Accelerated carbonation of reactive MgO and portland cement blends under flowing CO_2 gas. Cement and Concrete Composites 106: 468.

3. Coffetti D, Crotti E, Gazzaniga G, Carrara M, Pastore T, Coppola L (2022) Pathways towards sustainable concrete. Cem Conc Res, p. 154.

4. Shahbaz M, Balsalobre-Lorente D, Sinha A (2019) Foreign direct Investment-CO_2 emissions nexus in middle east and north african countries: Importance of biomass energy consumption. Journal of Cleaner Production 217: 603-614.

5. Yang KH, Jung YB, Cho MS, and Tae SH (2015) Effect of supplementary cementitious materials on reduction of CO_2 emissions from concrete. Journal of Cleaner Production 103: 774-783.

6. Juenger MCG, Siddique R (2015) Recent advances in understanding the role of supplementary cementitious materials in concrete. Cement and Concrete Research 78: 71-80.

7. Fode TA, Chande Jande YA, Kivevele T (2023) Effects of different supplementary cementitious materials on durability and mechanical properties of cement composite - Comprehensive review. Heliyon 9(7): e17924.

8. Shi C, Qu B, Provis JL (2019) Recent progress in low-carbon binders. Cement and Concrete Research 122: 227-250.

9. Cheng M, Wu L, Huang Y, Luo Y, Christie P (2014) Total concentrations of heavy metals and occurrence of antibiotics in sewage sludges from cities throughout China. Journal of Soils and Sediments 14(6): 1123-1135.

10. Lishan X, Tao L, Yin W, Zhilong Y, Jiangfu L (2018) Comparative life cycle assessment of sludge management: A case study of Xiamen, China. Journal of Cleaner Production 192: 354- 489.

11. Zhang J, Niu W, Yang Y, Hou D, Dong B (2022) Machine learning prediction models for compressive strength of calcined sludge-cement composites. Construction and Building Materials, p. 346.

12. Yang Y, Wang H, Li Z, Sun M, Zhang J (2024) Research on mechanical and durability properties of sintered sludge cement. Developments in the Built Environment 18: 100395.

13. Jamshidi A, Jamshidi M, Mehrdadi N, Shasavandi A, Pacheco-Torgal F (2012) Mechanical performance of concrete with partial replacement of sand by sewage sludge ash from incineration. Materials Science Forum 730-732: 462-467.

14. Karadumpa CS, Pancharathi RK (2021) Influence of particle packing theories on strength and microstructure properties of composite cement-based mortars. Journal of Materials in Civil Engineering 33: 10.

15. Lynn CJ, Dhir RK, Ghataora GS, West RP (2015) Sewage sludge ash characteristics and potential for use in concrete. Construction and Building Materials 98: 767-779.

16. Tipraj, Shanmugapriya T (2022) A comprehensive analysis on optimization of Sewage sludge ash as a binding material for a sustainable construction practice: A state of the art review. Materials Today: Proceedings 64: 1094-1101.

17. Wang L, Zou F, Fang X, Tsang DCW, Poon CS, et al. (2018) A novel type of controlled low strength material derived from alum sludge and green materials. Construction and Building Materials 165: 792-800.

18. Pan SC, Tseng DH, Lee CC, Lee C (2003) Influence of the fineness of sewage sludge ash on the mortar properties. Cement and Concrete Research 33(11): 1749-1754.

19. Chen Z, Poon CS (2017) Comparative studies on the effects of sewage sludge ash and fly ash on cement hydration and properties of cement mortars. Construction and Building Materials 154: 791-803.

20. Vilakazi S, Onyari E, Nkwonta O, Bwapwa JK (2023) Reuse of domestic sewage sludge to achieve a zero-waste strategy & improve concrete strength & durability - A review. South African Journal of Chemical Engineering 43: 122-127.

21. Rabie GM, El-Halim HA, Rozaik EH (2019) Influence of using dry and wet wastewater sludge in concrete mix on its physical and mechanical properties. Ain Shams Engineering Journal 10(4): 705-712.

22. Gu C, Ji Y, Zhang Y, Yang Y, Liu J, Ni T (2021) Recycling use of sulfate-rich sewage sludge ash (SR-SSA) in cement-based materials: Assessment on the basic properties, volume deformation and microstructure of SR-SSA blended cement pastes. Journal of Cleaner Production 282.

23. Cyr M, Coutand M, Clastres P (2007) Technological and environmental behavior of sewage sludge ash (SSA) in cement-based materials. Cement and Concrete Research 37(8): 1278-1289.

24. de Azevedo Basto P, Savastano H, de Melo Neto AA (2019) Characterization and pozzolanic properties of sewage sludge ashes (SSA) by electrical conductivity. Cement and Concrete Composites 104.

25. Suraneni P, Weiss J (2017) Examining the pozzolan city of supplementary cementitious 542 materials using isothermal calorimetry and thermogravimetric analysis. Cement and Concrete Composites 83: 273-278.

26. Mejdi M, Saillio M, Chaussadent T, Divet L, Tagnit-Hamou A (2020) Hydration mechanisms of sewage sludge ashes used as cement replacement. Cement and Concrete Research 135.

27. Lin KL, Chiang KY, Lin CY (2005) Hydration characteristics of waste sludge ash that is reused in eco-cement clinkers. Cement and Concrete Research 35(6): 1074-1081.

28. Krejcirikova B, Ottosen LM, Kirkelund GM, Rode C, Peuhkuri R (2019) Characterization of sewage sludge ash and its effect on moisture physics of mortar. Journal of Building Engineering 21: 396-403.

29. Bialowiec A, Janczukowicz W, Krzemieniewski M (2009) Possibilities of management of waste fly ashes from sewage sludge thermal treatment in the aspect of legal regulations. Rocznik Ochrona Srodowiska 11: 959-971.

30. Suraneni P, Hajibabaee A, Ramanathan S, Wang Y, Weiss J (2019) New insights from reactivity testing of supplementary cementitious materials. Cement and Concrete Composites 103: 331-338.

31. Darweesh HHM, Abu-El-Naga H (2024) The performance of portland cement pastes (OPC) incorporated with Ceramic Sanitary Ware Powder Waste (CSPW) at ambient temperature. Sustainable Materials Processing and Management 4(1): 56-70.

32. Darweesh HHM, Abu-El-Naga H (2024) Effect of curing temperatures on the hydration of cement pastes containing nanograin size particles of sanitary ware ceramic powder waste. International Journal of Materials Science 5(1): 07-14.

33. Naamane S, Rais Z, Taleb M (2016) The effectiveness of the incineration of sewage sludge on the evolution of physicochemical and mechanical properties of Portland cement. Construction and Building Materials 112: 783-789.

34. Ottosen LM, Thornberg D, Cohen Y, Stiernström S (2022) Utilization of acid-washed sewage sludge ash as sand or cement replacement in concrete. Resources, Conservation and Recycling 176: 105943.

35. Motisariya K, Agrawal G, Baria M, Srivastava V, Dave DN (2023) Experimental analysis of strength and durability properties of cement binders and mortars with addition of microfine sewage sludge ash (SSA) particles. Materials Today: Proceedings 85: 24-28.

36. Hewlett PC, Liska M (2019) Pozzolanas and pozzolanic materials. In: Lea's chemistry of cement and concrete (5th edn), Butterworth-Heinemann, pp. 363-467.

37. ASTM C187 (1998) Test method for amount of water required for normal consistency of hydraulic cement paste. American Society for Testing and Materials.

38. ASTM C191-21 (1998) Standard test methods for time of setting of Hydraulic cement by Vicat Needle. West Conshohocken, ASTM International, PA, USA, pp. 8-10.

39. ASTM C642-21 (2021) Standard test method for density, absorption, and voids in hardened concrete. West Conshohocken, ASTM International, PA, USA, p. 3.

40. Darweesh HHM (2020) Specific characteristics and microstructure of Portland cement pastes containing wheat straw ash (WSA). Indian Journal of Engineering17(48): 569-583.

41. ASTM C293-02 (2002) Standard test method for flexural strength of concrete (using simple beam with center point loading). American Society for Testing and Materials.

42. ASTM C348-21 (2021) Standard test method for flexural strength of hydraulic-cement mortars. ASTM International, West Conshohocken, PA, USA.

43. ASTM C109-20 (2020) Standard test method for compressive strength of hydraulic cement mortars. ASTM International, West Conshohocken, PA, USA.

44. Darweesh HHM (2024) Performance of brick demolition waste in Geopolymer cement pastes. International Journal of Civil Engineering and Architecture Engineering 5(1): 34-44.

45. Darweesh HHM (2024) Reactive magnesia Portland blended cement pastes. Journal of Civil Engineering and Applications 5(1): 23-32.

46. Darweesh HHM (2023) Utilization of oyster shell powder for hydration and mechanical properties improvement of portland cement pastes. Journal of Sustainable Materials Processing and Management 3(1): 19-30.

47. Darweesh HHM (2020) Characteristics of portland cement pastes blended with silica nanoparticles. To Chemistry 5: 1-14.

48. Darweesh HHM (2020) Physico-mechanical properties and microstructure of Portland cement pastes replaced by corn stalk ash (CSA). International Journal of Chemical Research and Development 2(1): 24-33.

49. Coffetti D, Crotti E, Gazzaniga G, Carrara M, Pastore T, et al. (2022) Pathways towards sustainable concrete. Cement Concr Res 154: 106718.

50. Wang J, Che Z, Zhang K, Fan Y, Niu D, et al. (2023) Performance of recycled aggregate concrete with supplementary cementitious materials (fly ash, GBFS, silica fume, and metakaolin): mechanical properties, pore structure, and water absorption. Constr Build Mater 368: 130455.

51. Fakhri RS, Dawood ET (2023) Influence of binary blended cement containing slag and limestone powder to produce sustainable mortar. AIP Conf Proc 2862(1): 020028.

52. Sagade A, Fall M (2024) Study of fresh properties of cemented paste backfill material with ternary cement blends. Construct Build Mater 411: 134287.

53. Mahmoodi O, Siad H, Lachemi M, Dadsetan S, Sahmaran M (2020) Development of ceramic tile waste geopolymer binders based on pre-targeted chemical ratios and ambient curing. Construction and Building Materials 258: 120297.

54. Wu H, Gao J, Liu C, Zhao Y, Li S (2024) Development of nano-silica modification to enhance the micro-macro properties of cement-based materials with recycled clay brick powder. Journal of Building Engineering 86: 108854.

55. Tanash AO, Muthusamy K, Mat Yahaya F, Ismail MA (2023) Potential of recycled powder from clay brick, sanitary ware, and concrete waste as a cement substitute for concrete: An overview. Construction and Building Materials 401: 132760.

56. Tian B, Ma W, Li X, Jiang D, Zhang C, Xu J, et al. (2023) Effect of ceramic polishing waste on the properties of alkali-activated slag pastes: Shrinkage, hydration and mechanical property. Journal of Building Engineering 63: 105448.

57. Chen G, Li S, Zhao Y, Xu Z, Luo X, Gao J, et al. (2023) Hydration and microstructure evolution of a novel low carbon concrete containing recycled clay brick powder and ground granulated blast furnace slag. Construction and Building Materials 386: 131596.

58. Likes L, Markandeya A, Haider MM, Bollinger D, McCloy JS, Nassiri S, et al. (2022) Recycled concrete and brick powders as supplements to Portland cement for more sustainable concrete. Journal of Cleaner Production 364: 132651.

59. Li S, Chen G, Zhao Y, Xu Z, Luo X, Liu C, et al. (2023) Investigation on the reactivity of recycled brick powder. Cement and Concrete Composites 139: 105042.

60. Jain P, Gupta R, Chaudhary S (2022) Comprehensive assessment of ceramic ETP sludge waste as a SCM for the production of concrete. Journal of Building Engineering 57: 104973.

61. Al-Shmaisani S, Kalina RD, Ferron RD, Juenger MCG (2022) Critical assessment of rapid methods to qualify supplementary cementitious materials for use in concrete. Cem Concr Res 153: 106709.

62. Tian B, Ma W, Li X, Jiang D, Zhang C, Xu J, et al. (2023) Effect of ceramic polishing waste on the properties of alkali-activated slag pastes: Shrinkage, hydration and mechanical property. Journal of Building Engineering 63: 105448.

63. Jain P, Gupta R, Chaudhary S (2022) Comprehensive assessment of ceramic ETP sludge waste as a SCM for the production of concrete. Journal of Building Engineering 57: 104973.

64. Darweesh HHM (2016) Ceramic wall and floor tiles containing local waste of cement kiln dust- Part II: Dry and firing shrinkage as well as mechanical properties. American Journal of Civil Engineering and Architecture 4(2): 44-49.

65. Zhang Y, Çopuroglu˘ O (2024) Correlation between slag reactivity and cement paste properties: the influence of slag chemistry. J Mater Civ Eng 36(3): 04023618.

66. Azevedo ARG, Marvila TM, Júnior Fernandes W, Alexandre J, Xavier GC, et al. (2019) Assessing the potential of sludge generated by the pulp and paper industry in assembling locking blocks. J Build Eng 23: 334-340.

67. Zhang Y, Çopuroglu˘ O (2024) Correlation between slag reactivity and cement paste properties: the influence of slag chemistry. J Mater Civ Eng 36(3): 04023618.

68. Azevedo ARG, Marvila TM, Júnior Fernandes W, Alexandre J, Xavier GC, et al. (2019) Assessing the potential of sludge generated by the pulp and paper industry in assembling locking blocks. J Build Eng 23: 334-340.

69. Jain P, Gupta R, Chaudhary S (2022) Comprehensive assessment of ceramic ETP sludge waste as a SCM for the production of concrete. Journal of Building Engineering 57: 104973.

70. El-Dieb AS, Kanaan DM (2018) Ceramic waste powder an alternative cement replacement - characterization and evaluation. Sustainable Materials and Technologies 17: e00063.

71. Azevedo A, de Matos P, Marvila M, Sakata R, Silvestro L, et al. (2021) Hydration, and microstructure of Portland cement pastes produced with ground Açaí fibers. Applied Sciences.

72. Darweesh HHM, El-Suoud MA (2019) Influence of sugarcane bagasse ash substitution on portland cement characteristics. Indian J Eng 16: 252-266.

73. Darweesh HHM, El-Suoud MA (2020) Palm ash as a pozzolanic material for portland cement pastes. To Chemistry Journal, 4: 72-85.

74. Steiner LR, Bernardin AM, Pelisser F (2015) Effectiveness of ceramic tile polishing residues as supplementary cementitious materials for cement mortars. Sustainable Materials and Technologies 4: 30-35.

75. Darweesh HHM (2020) Influence of sunflower stalk ash (SFSA) on the behavior of portland cement pastes. Results in Engineering 8: 100171.

76. Darweesh HHM (2021) Low heat blended cements containing nanosized particles of natural pumice alone or in combination with granulated blast furnace slag. Nano Prog 3(5): 38-46.